PERGAMON

Atmospheric Environment 36 (2002) 421–434

ATMOSPHERIC ENVIRONMENT

www.elsevier.com/locate/atmosenv

Quantification on source/receptor relationship of primary pollutants and secondary aerosols from ground sources—Part II. Model description and case study

Chien-Lung Chen[a], Ben-Jei Tsuang[a,*], Rong-Chang Pan[a], Chia-Ying Tu[a], Jen-Hui Liu[a], Pei-Ling Huang[a], Hsunling Bai[b], Man-Ting Cheng[a]

[a] *Department of Environmental Engineering, National Chung-Hsing University, Taichung 40227, Taiwan, ROC*
[b] *Institute of Environmental Engineering, National Chiao-Tung University, Hsin-Chu, Taiwan, ROC*

Received 26 January 2001; received in revised form 12 September 2001; accepted 19 September 2001

Abstract

A Circuit Trajectory transfer-coefficient model (CTx) is developed in this study based on the parameterization presented in a companion paper (Tsuang et al., Atmos. Environ., in this issue). CTx was tested by applying it to Metropolitan Taipei for the entire year 1998. The model was calibrated in January and verified throughout the year. The results indicate that the correlation coefficients (r) for daily concentrations of CO, NO_x, SO_2, $PM_{2.5}$ and PM_{10} were 0.75, 0.69, 0.39, 0.55 and 0.55, respectively, with biases of the means ranging from 0% to 20% during the verification period. According to contour plots of contributed concentrations to the city, "teleconnections" between source emissions and their contributions to the city can be identified. In addition, the model captures most of the dust episodes except during the periods of Asian dust storms. The sensitivity analysis shows that the calculated PM_{10} concentration is most sensitive to its dry deposition velocity as well as its emission rate. A more thorough study on the deposition velocity of $PM_{2.5}$ is suggested.

Keywords: Transfer coefficient; Trajectory; Contributed concentration; Particulate matter; Sensitivity test; Taipei; Dust storm

1. Introduction

A Circuit Trajectory transfer-coefficient model (CTx) is developed in this study based on a theory for determining the transfer-coefficient presented in a companion paper (Tsuang et al., 2002). In the following sections, we describe the model structure and the parameterizations used in this model. Then, the model is applied to Metropolitan Taipei as a case study. Metropolitan Taipei is located in northern Taiwan, where rawinsonde data and intense surface meteorological data are continuously monitored and elevated sources are fewer in number. Hourly concentrations of CO, NO_x, SO_2, $PM_{2.5}$ (particles whose sizes are $<2.5\,\mu m$ in diameter) and PM_{10} (particles whose sizes are $<10\,\mu m$ in diameter) are simulated and compared. In addition, we examine the sensitivity of calculated concentrations to a variety of model parameters and inputs. Then, we show that placing the emission rate in time series can improve the simulation in general. Finally, we discuss the application of the model for estimating the contributed concentrations of sources to Metropolitan Taipei during a PM_{10} episode day and a non-episode day.

2. Model description

2.1. Trajectories

In CTx, back-trajectories for a selected time (default 24 h) of transport were computed according to wind

*Corresponding author. Tel.: +886-4-22851206; fax: +886-4-22862587.
E-mail address: tsuang@nchu.edu.tw (B.-J. Tsuang).

1352-2310/02/$ - see front matter
PII: S1352-2310(01)00492-7

data. There were three trajectories to the receptor (left, central and right). Each trajectory grid had a width of 10 km (i.e. $\Delta y = 10$ km). Trajectories were calculated using observed surface wind fields and adjusted to a selected height according to a log-vertical profile of wind speed. In addition, the minimum wind speed was set to be $1\,\mathrm{m\,s^{-1}}$. The wind field along a trajectory was established in two steps: First, it was determined by the interpolation of observed wind data using the square of inverse-distance weighting method (US/EPA, 1994). Then, the interpolated wind field was further adjusted according to the channel effect of terrain (Scire et al., 2000; Tsuang et al., 2000). According to the weighting, the interpolated wind field along a trajectory was influenced most significantly by a nearby meteorological station data.

Once the trajectory paths were computed, the meteorological conditions along the path at each time step were extracted from the corresponding grid using the same interpolation method including air temperature, relative humidity, atmospheric pressure, wind speed, wind direction, cloud fraction, zenith angle and rain duration time.

2.2. Mixing height and stability

A Lagrangian model based on Tu (1999) is used to calculate the mixing heights and stabilities along the trajectory, where the land parameters are determined according to Tsuang and Tu (2001). Input data of relative humidity, pressure, wind vector, cloud fraction, zenith angle, rain duration time and lapse rate above a mixing height are used to run the sub-model. All the meteorological data were obtained by interpolating among the surface meteorological stations along the central trajectory, except for the lapse rate above a mixing height. Lapse rate above a mixing height is either set at a default value of the wet lapse rate ($=-0.65\,\mathrm{K\,km^{-1}}$) or calculated according to rawinsonde data provided by users. The Lagrangian model parameterizes the mixing height according to Holzworth (1972).

2.3. Dry deposition, scavenging coefficient and gas–particle conversion rates

Similar to Lurmann et al. (1997), the dry deposition rates for gases were calculated based on a three-resistance dry deposition algorithm by Padro et al. (1991) and US EPA (1995), and those rates for all particles were calculated based on Slinn and Slinn (1980). Scavenging coefficients (Λ) for particle and SO_2 were calculated by taking into account the precipitation rate according to Scott (1982), Kessler (1969), Seinfeld and Pandis (1998) and Uijlenhoet and Stricker (1999). The rest of gas scavenging coefficients for CO and NO_x were assigned as $9.0\mathrm{E}{-12}\,\mathrm{s^{-1}}$ and $1.4\mathrm{E}{-10}\,\mathrm{s^{-1}}$, respectively (Hertel et al., 1995). The gas–particle conversion rate of particulate sulfate from gaseous SO_2 was set at $5\%\mathrm{S\,h^{-1}}$ and that of particulate nitrate from NO_x was set at $1.5\%\mathrm{N\,h^{-1}}$ (Kuo et al., 1996). With respect to the size category of secondary aerosol, 85% of gaseous SO_2 converted sulfate and 58% of gaseous NO_x converted nitrate are set to be in the radii of $PM_{2.5}$ and the rests remain in $PM_{2.5-10}$ according to the field data in a coastal area of Taiwan (Tsai and Cheng, 1999). The density of particulate matter is set to be $2200\,\mathrm{kg\,m^{-3}}$ (Juozaitis et al., 1996; Chate and Kamra, 1997). Parameters in the above references relevant to this study are listed in Table 1. The same parameters have been tested for the simulation of air pollutants with a Gaussian-type model in Taichung, where the measurements of sulfate aerosol and nitrate aerosol are available (Tsuang et al., submitted).

3. Taipei case study

Taipei City is the largest city in Taiwan. It has 2.6 million inhabitants. The population increases to 8.3 million people if the neighborhood counties of Taipei County, Keelung City and Taoyuan County are included (MOI, 2001). Taipei City is an ideal place in Taiwan to test the CTx model because the construction of new factories is not allowed and old factories were forced to relocate 20 years ago. Consequently, elevated sources are fewer in number. Note that the algorithm to calculate the transfer coefficients in CTx is valid only for ground sources.

Applying the model to Taipei City, we chose the air quality station at Ku-Ting as the receptor. The study period chosen was 1998, the first year when both the concentrations of PM_{10} and $PM_{2.5}$ were measured and available simultaneously. Hourly concentrations of CO, NO_x, SO_2, $PM_{2.5}$ and PM_{10} at Ku-Ting station, measured continuously by the Environmental Protection Agency in Taiwan (EPA/ROC), were used in the study. Fig. 1 shows the location of the air quality station, the meteorological stations and the distribution of PM_{10} emissions rate used in the study. The region is characterized by complex terrain. Notable land–sea breezes, uphill–downhill winds and a monsoon climate cause significant diurnal and seasonable variability in weather conditions. In the winter, the prevailing wind comes from the northeast, and in the summer, the prevailing wind comes from the southwest. The initial concentrations of pollutants at the receptor for each month of the simulated period and the boundary condition for the concentrations at the beginning of the 24 h trajectory were set at their observed values.

Table 1
Parameters in CTx

Parameters	Value
Particle	
Density[a]	2200 kg m^{-3}
Fine particle diameter (<2.5 μm)	2.4 μm
Coarse particle diameter (2.5–10 μm)	4.5 μm
Scavenging coefficients	Scott (1982)
dry deposition velocity	Slinn and Slinn (1980)
Gas	
Mass fraction between radii of 2.5 and 10 μm of SO_2 converted sulfate (f_{Sul})[b]	85%
Mass fraction between radii of 2.5 and 10 μm of NO_x converted nitrate (f_{Nit})[b]	58%
SO_2 scavenging coefficients	Seinfeld and Pandis (1998)
NO_x scavenging coefficients[c]	1.4E−10 s^{-1}
CO scavenging coefficients[c]	9.0E−12 s^{-1}
Gas–particle conversion rate of SO_2[d]	5.0%S h^{-1}
Gas–particle conversion rate of NO_x[d]	1.5%N h^{-1}
Dry deposition velocity	Padro et al. (1991) and US EPA (1995)

[a] Juozaitis et al. (1996), Chate and Kamra (1997).
[b] Tsai and Cheng (1999).
[c] Hertel et al. (1995).
[d] Kuo et al. (1996).

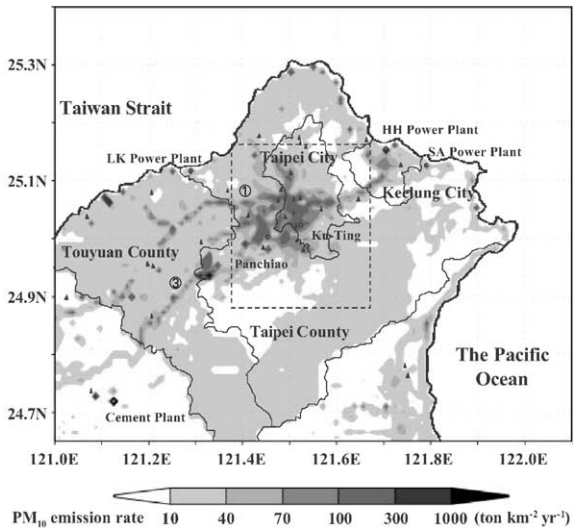

Fig. 1. Locations of the Ku-Ting monitoring station, Panchiao air sounding station, the largest PM_{10} emission source (i.e. cement plant), the first three largest SO_2 emission sources (i.e. three coal-fueled power plants), two highways #1 and #3, meteorological stations (triangle) and distribution of PM_{10} emission rate in the northern Taiwan. The rectangular area represents a region of $30 \times 30\,km^2$ centered on Ku-Ting station.

3.1. Emissions

Table 2 summarizes the emissions inventory in 1997 by CTCI (1999) in a region $10 \times 10\,km^2$ and $30 \times 30\,km^2$ centered at Ku-Ting station and four major stationary sources in the neighborhood counties. It shows that in the region of $10 \times 10\,km^2$ and of $30 \times 30\,km^2$ most of the pollutants, except SO_2, were dominated by ground sources, especially CO emissions. Up to 99% of CO emissions were from ground sources.

The emissions inventory by CTCI (1999) is only available in annual average. In order to take into account the day-of-the week variability (DOWV), an index was introduced for parameterization of the short-term variability of emissions and especially the traffic (Ziomas et al., 1995; Simmonds and Keay, 1997; Cheng and Lam, 1998). The values of this index are presented in Table 3. The index was determined according to the DOWV of concentration levels at Ku-Ting station for the period 1994–1999. There is no significant difference in the values of the index from Monday to Saturday because of 6-day workweeks in Taiwan.

3.2. Meteorological data

Surface wind data were observed by either Central Weather Bureau (CWB/ROC) or EPA/ROC. Back-trajectories at 100 m height for 24 h of transport were computed according to the wind data. The temporal resolution of the observed wind data was 1 h and the spatial resolution was about 10 km. Since the temporal and the spatial resolutions of the wind data were much denser than those by Kahl and Samson (1986), Draxler (1987) and Rolph and Draxler (1990), the derived trajectories should be less problematic (Stohl, 1998).

Table 2
Emissions inventory in 1997 in the region of $10 \times 10\,km^2$ and $30 \times 30\,km^2$ centered at Ku-Ting station and major stationary sources

Sources			Emission rate (ton yr^{-1})			
			CO	NO_x	SO_2	PM_{10}
$10 \times 10\,km^2$						
Elevated source			54 (<0.1%)	345 (2.7%)	534 (22.0%)	27 (0.3%)
Ground source			130,981 (99.9%)	12,192 (97.3%)	1893 (78.0%)	8481 (99.7%)
$30 \times 30\,km^2$						
Elevated source			432 (0.1%)	5593 (12.5%)	3922 (40.5%)	884 (2.7%)
Ground source			400,092 (99.9%)	39,246 (87.5%)	5761 (59.5%)	32,337 (97.3%)
Major stationary sources[a]	Distance to the receptor					
HH power plant[a]	25.5 km	NE	—	8781	23,138	1303
SA power plant[a]	31.4 km	ENE	162	2612	7138	125
LK power plant[a]	25.2 km	WNW	139	6056	4511	155
AH cement plant[a]	51.6 km	SW	1559	4082	156	6930

[a] HH: Hsieh-Ho coal-fueled power plant, SA: Shen-Ao coal-fueled power plant, LK: Lin-Kou coal-fueled power plant, AH: Asia-Hsinchu cement plant.

Table 3
The index characterizing the short-term variability of the emissions based on the day-of-the week variability (DOWV) analysis on the concentration levels of Ku-Ting station 1994–1999

Day	CO	NO_x	SO_2	$PM_{2.5}$	$PM_{2.5-10}$
Monday	1.03	1.02	1.00	0.99	0.97
Tuesday	1.02	1.03	1.05	0.99	1.07
Wednesday	1.02	1.03	1.05	0.99	1.06
Thursday	1.03	1.04	1.04	1.03	1.10
Friday	1.03	1.03	1.05	1.01	1.01
Saturday	1.03	1.02	1.00	1.03	0.97
Sunday	0.85	0.85	0.81	0.94	0.81

Such a temporal resolution was able to capture the diurnal variation of wind direction in the study site. Lapse rate above a mixing height is obtained from rawinsonde data at Panchiao, about 9 km to the southwest and maintained by CWB/ROC.

3.3. Calibration

Since many parameters as well as the emission inventory are subject to particular uncertainties, calibration is usually necessary for applying air quality to a case study. We use the data of January 1998 for the calibration. Parameters calibrated by month will be applied to the rest of the year for the verification. First, we perform a sensitivity analysis to understand which parameters are the important parameters for the simulation. Sensitivity tests of the calculated concentrations to emission inventories, gas–particle conversion rates, dry deposition velocity, size fractions of gas converted second aerosols and scavenging coefficients are discussed (Chang et al., 1996; Jacobson, 1997b; Schwede and Paumier, 1997). The results are listed in Table 4. A sensitivity index SI in the table defined as (Yang et al., 1997)

$$\mathrm{SI} = \left(\frac{f(x+\Delta x) - f(x)}{f(x)}\right) \Big/ \left(\frac{\Delta x}{x}\right) \quad (1)$$

is used to identify the key parameters, where x is one of the parameters, $f(x)$ is the calculated result using the parameter x, and Δx is a perturbation of x. The larger the magnitude of the SI, the more important the parameter is. A negative SI indicates that the calculated concentrations decrease with the parameter. The table shows that the calculated PM_{10} concentrations are the most sensitive to the rate of the PM_{10} dry deposition velocity and then to the rate of the primary PM_{10} emission. Note that SI of the deposition rate is −118% and that of the emission rate is 91%. The PM_{10}

Table 4
Sensitivity Index of the calculation of the concentrations to emission inventories, gas-particle conversion rates, dry deposition velocities, trajectory height and scavenging coefficients in Taipei, January 1998

Parameters and inputs	Sensitivity index (%)				
	CO	NO_x	SO_2	$PM_{2.5}$	PM_{10}
Jan 1998					
Half particle emissions	0	0	0	88	91
Half SO_2 emissions	0	0	100	6	4
Half NO_x emissions	0	100	0	5	4
Half CO emissions	100	0	0	0	0
Half dry deposition velocity	−74	−112	−123	−117	−118
Half SO_2 conversion rate	0	0	−6	6	4
Half NO_x conversion rate	0	−1	0	5	4
Half the fine particle fraction of SO_2 converted sulfate (f_{Sul})	0	0	0	6	2
Half the fine particle fraction of NO_x converted nitrate (f_{Nit})	0	0	0	5	1
Double trajectory height (at 200 m)	−8	−3	9	−5	−5
Raining day (11 days) in Jan 1998					
Half particle scavenging coeff.	0	0	0	−12	−11
Half SO_2 scavenging coeff.	0	0	−12	−1	−0
Half NO_x scavenging coeff.	0	0	0	0	0
Half CO scavenging coeff.	0	0	0	0	0

concentrations are less sensitive to the gas–particle conversion rates, the trajectory height and the size fraction of converted second aerosols. The magnitudes of the SIs of these parameters are $<5\%$. Similarly, it is found that CO, NO_x, SO_2 and $PM_{2.5}$ are most sensitive to their emission rates and dry deposition velocities. On rainy days, the scavenging coefficients of PM_{10} and SO_2 are also important in determining their concentrations with SIs of about -12%. In contrast, SIs of the scavenging coefficients of NO_x and CO are about 0% and have little influence in determining their concentrations. Moreover, both the emission inventories (Tsuang and Chao, 1999; Chang et al., 2000; Kuang, 2000) and the dry deposition velocities over a complex terrain (Wesely and Hicks, 2000) are suspected of having of high uncertainty. Therefore, only these two dominant parameters are calibrated. Errors in the other terms are difficult to calibrate. However, Table 4 shows that they are not significant, and we do not calibrate them. It is worth knowing that these parameters alter mainly the magnitudes of the calculated concentrations with minor effects on improving the correlation coefficients. The correlation coefficients vary mainly with meteorological conditions and then with the variations of the emissions in time.

Next, we multiplied the dry deposition velocities calculated according to Wesely (1989) and Slinn and Slinn (1980) by a factor of 5, namely the exposure area ratio (EAR) of Metropolitan Taipei, in order to account for extra surfaces in Taipei for deposition. In urban areas, pollutants can be deposited on the sides of buildings in addition to roof surfaces. The current dry deposition schemes applied for complex terrain and urban areas are less reliable than those for flat areas (Wesely and Hicks, 2000). In addition to the EAR, the dry deposition rate for $PM_{2.5}$ has been further calibrated by doubling the rate according the result of another study site (Tsuang et al., 2001b). Note that the uncertainty of the dry deposition of the fine diameter has at least an order of magnitude (Seinfeld and Pandis, 1998). Finally, the emission rates of CO, NO_x, SO_2, $PM_{2.5}$ and $PM_{2.5-10}$ (particles 2.5–10 μm in diameter) were scaled down by factors of 0.66, 0.63, 0.35, 0.91 and 0.41, respectively, to reach closer means of concentrations for each pollutant between observation and calculation during the calibration period. Table 5 summarizes the results of the simulations using the original and the calibrated parameters. No significant changes were found in the correlation coefficients but the biases have been reduced. The correlation coefficients of the calibration month for CO, NO_x, SO_2, $PM_{2.5}$ and PM_{10} are 0.38, 0.53, 0.26, 0.49 and 0.54, respectively.

3.4. Verification

The calibrated emission inventory and dry deposition velocities are applied to February–December 1998 for verification. The results of the simulation are summarized in Table 6. The calculated and observed daily concentrations of CO and PM_{10} are shown in Figs 2 and 3. They show that the simulations for CO, NO_x, and SO_2 are satisfactory. No significant biases occur. The results indicate that the correlation coefficients (r) for daily concentrations of CO, NO_x, SO_2, $PM_{2.5}$ and PM_{10}

Table 5
Statistics of original and calibrated daily CO, NO_x, SO_2, $PM_{2.5}$ and PM_{10} concentrations in Taipei, Taiwan, January 1998[a]

Pollutant	Obs	Calc	Corr. coeff. (r)	RMSE	Bias (%)	nos (a)	noo (b)	nou (c)	noe	EAR/ $a/(a+b+c)$ (%)
Original										
CO (ppm)	1.148	1.750	0.38	0.841	52.4	18	12	1	5	58
NO_x (ppb)	57.4	90.6	0.53	40.7	57.8	17	14	0	6	55
SO_2 (ppb)	3.7	10.6	0.26	8.0	186.5	8	23	0	7	26
$PM_{2.5}$ ($\mu g\,m^{-3}$)	38.6	46.2	0.52	14.3	19.7	21	7	3	7	68
PM_{10} ($\mu g\,m^{-3}$)	51.1	76.2	0.54	36.2	49.1	22	9	0	6	71
Calibrated										
CO (ppm)	1.148	1.156	0.38	0.446	0.7	23	4	4	5	74
NO_x (ppb)	57.4	57.1	0.53	18.6	-0.5	25	1	5	6	81
SO_2 (ppb)	3.7	3.7	0.26	2.2	0.0	23	1	7	7	74
$PM_{2.5}$ ($\mu g\,m^{-3}$)	38.6	38.5	0.49	11.2	-0.3	25	1	5	7	81
PM_{10} ($\mu g\,m^{-3}$)	51.1	51.0	0.52	21.3	0.2	25	1	5	6	81

[a] RMSE: root-mean-square error. Bias = (mean C_p − mean C_o)/mean C_o, where C_p and C_o are the predicted and observed concentrations. nos: number of successful times in simulating the periods of episode days or non-episode days, where the episode day is defined to be the day when the concentration is higher than the mean of the study period plus one standard deviation. noo: number of non-episode days when the concentrations are overestimated as episode days. nou: number of episode days when the concentrations are underestimated as non-episode days. noe: number of observed episode days. EDR: episode-distinguished ratio.

Table 6
Statistics of daily CO, NO_x, SO_2, $PM_{2.5}$ and PM_{10} concentrations in Taipei, Taiwan, February–December 1998

Pollutant	Obs	Calc	Corr. coeff. (r)	RMSE	Bias (%)	nos (a)	noo (b)	nou (c)	noe	EAR/ $a/(a+b+c)$ (%)
CO (ppm)	1.099	1.147	0.75	0.276	4.4	282	27	17	54	87
NO_x (ppb)	54.6	57.0	0.69	14.8	4.4	286	10	29	50	88
SO_2 (ppb)	3.4	3.4	0.39	1.8	0.0	272	12	38	44	85
$PM_{2.5}$ ($\mu g\,m^{-3}$)	32.2	38.4	0.55	14.1	19.3	243	50	16	44	79
PM_{10} ($\mu g\,m^{-3}$)	42.7	49.7	0.55	20.9	16.4	247	30	21	37	83

were 0.75, 0.69, 0.39, 0.55 and 0.55, respectively. This shows that the simulated CO had the highest correlation and the simulated SO_2 had the lowest correlation. The results are reasonable since, among these pollutants, CO had the largest portion of emissions from ground sources and SO_2 had the lowest portion. Note again that the algorithms derived in the theory section are only valid for ground sources. Nonetheless, the table shows that the mean of $PM_{2.5}$ concentrations was overestimated by $10\,\mu m\,m^{-3}$ particularly from May to August. At this stage, it is unclear which model errors caused errors in the response. One likely reason is that the dry deposition algorithm for particulates with size $<2.5\,\mu m$ is too low under light wind conditions. Note that in these months in Taipei, the mean wind speed was $2\,m\,s^{-1}$, and in the other months, the mean speed was $3\,m\,s^{-1}$.

An episode-distinguished ratio EDR is proposed here for evaluating the capability of a model in distinguishing between the episode and non-episode days. It is defined as

$$\mathrm{EDR} = \frac{\mathrm{nos}}{\mathrm{nos} + \mathrm{noo} + \mathrm{nou}}, \tag{2}$$

where nos is the number of successful times in simulating the periods of episode days or non-episode days; noo is the number of non-episode days when the concentrations are overestimated as episode days; and nou is the number of episode days when the concentrations are underestimated as non-episode days. The episode day is defined as the day when the concentration is higher than the mean of the study period plus one standard deviation. The numerator of the EDR represents the number of successful predictions of the periods of episodes or non-episode days. The denominator of the EDR represents the total days of the prediction.

Table 6 shows that the model is capable of distinguishing between episode and non-episode days ranging

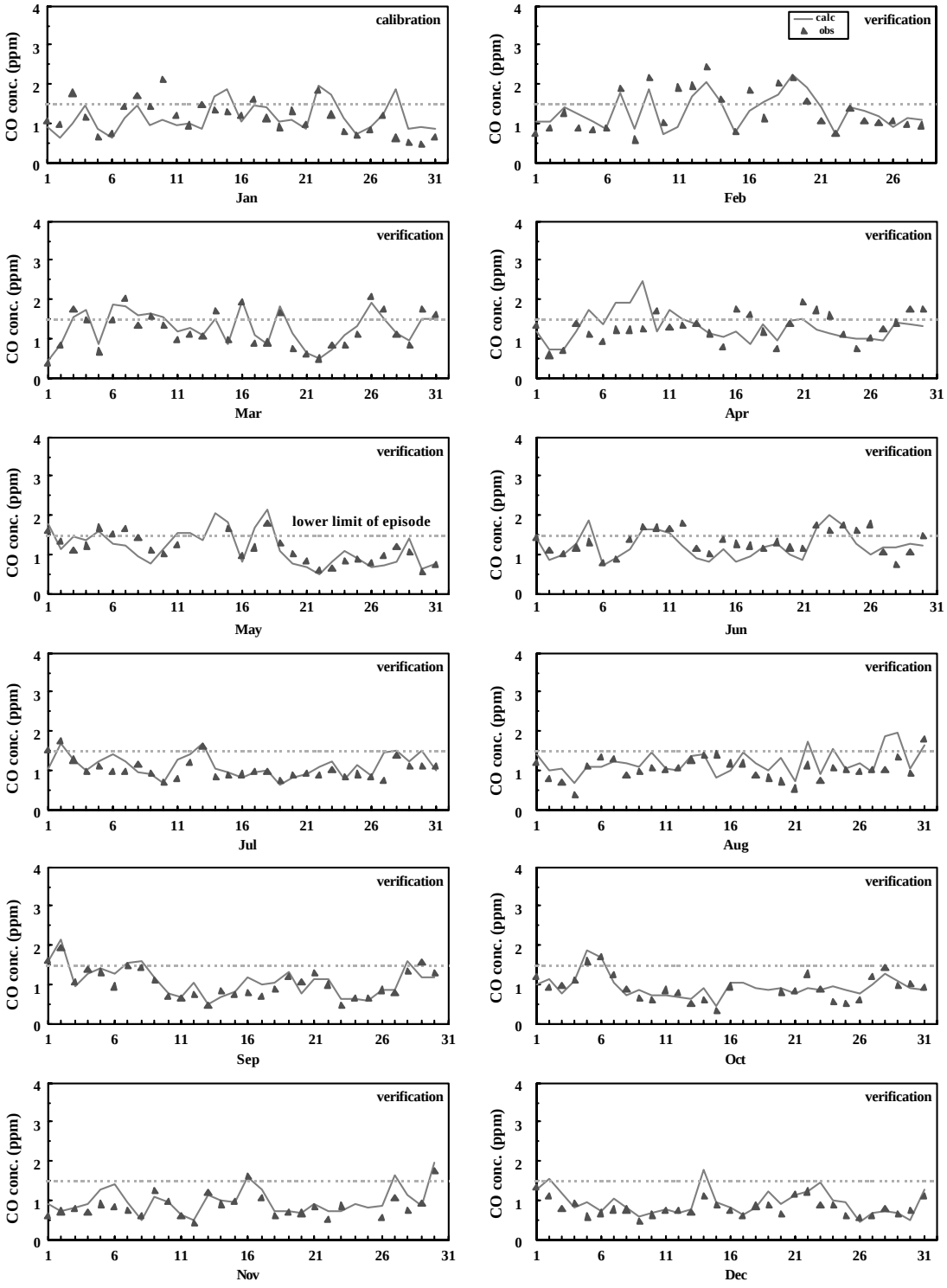

Fig. 2. CO daily concentrations at Ku-Ting station, Taiwan, 1998. (solid lines represent calculated concentrations and symbols observed data).

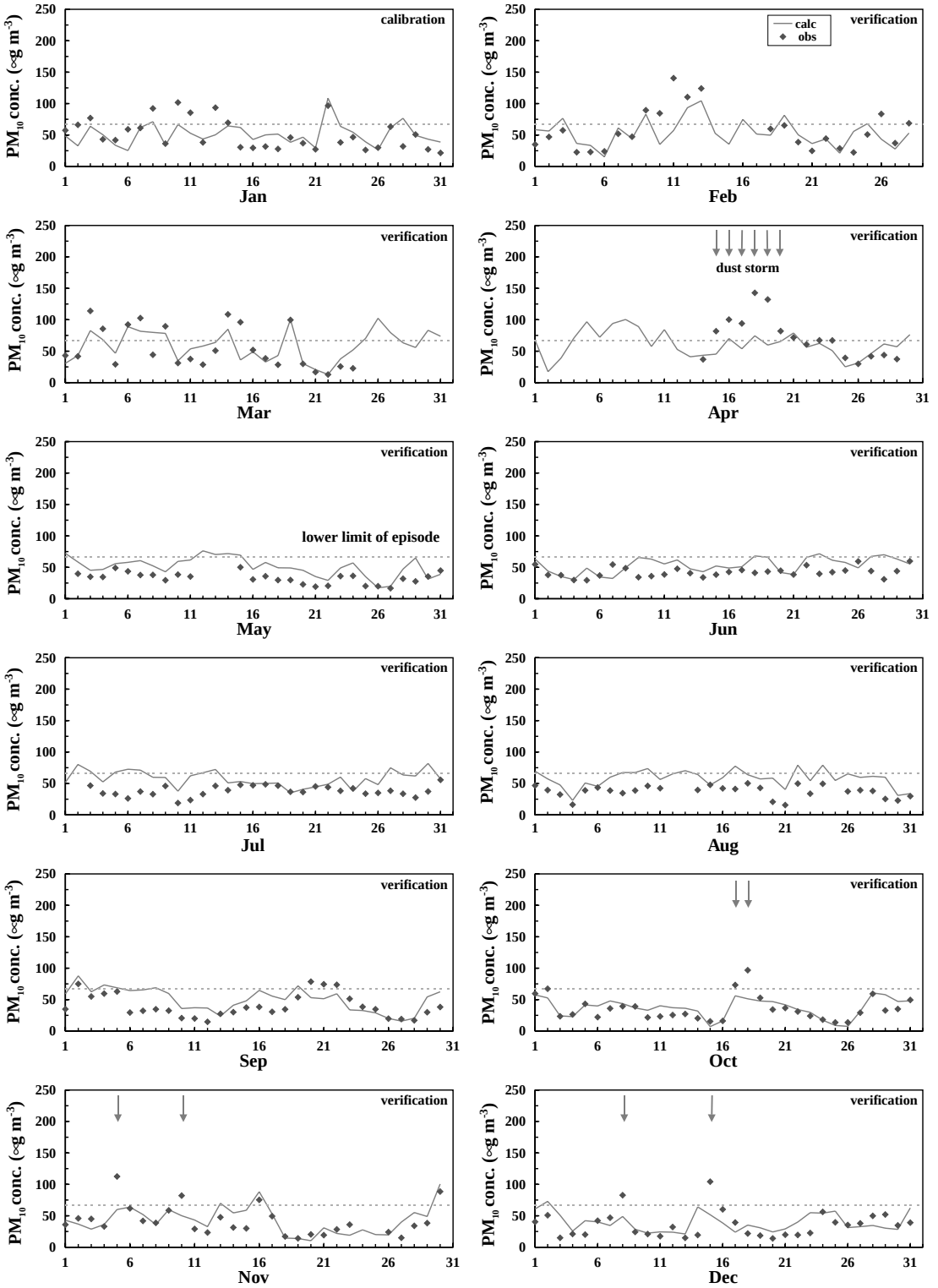

Fig. 3. PM_{10} daily concentrations at Ku-Ting station, Taiwan, 1998. Arrows on the top of each graph represent Asia dust storm periods identified by Chang and Wu (2001). (solid lines represent calculated concentrations and symbols observed data).

from 79% to 88% varying with pollutants. The skills in CO, NO_x and SO_2 are higher than $PM_{2.5}$ and PM_{10}. Most of the episodes occurred from November to April. The overestimation of the $PM_{2.5}$ concentration in the summer deteriorates the EDR of $PM_{2.5}$. With respect to PM_{10}, the criterion of PM_{10} is its concentration higher than $66\,\mu g\,m^{-3}$. There were 44 PM_{10} episodes in 1998. The model captures 19 episodes but falsely reports 31 additional episodes. Most of the falsely reported episodes occurred under light wind conditions. With respect to the uncaptured 25 PM_{10} episodes, the periods of 12 of the 25 episodes (15–20 April, 17–18 October, 5 and 10 November, 8 and 15 December) corresponded with periods when Asian dust storms affected Taiwan. Fig. 3 also shows the periods identified by Chang and Wu (2001) when Taiwan was affected by Asian dust storms. The dust storms carry much dust of coarse radii (radii in the range 2.5–10 μm) from desert regions in northern China. Transported long distances, they are known to subside over Taiwan during the synoptic weather pattern governed by a cold front passage or a strong anticyclone (Chen and Chen, 1987). Note that during the 12 suspected Asia dust storm episodes, coarse particles dominated and the ratios of the concentrations between $PM_{2.5}$ and PM_{10} were relatively low (Fig. 4).

4. Discussion

4.1. Source/receptor relationship

4.1.1. An episode day

On 8 January 1998, a PM episode occurred in which the daily average of PM_{10} was $92\,\mu g\,m^{-3}$, exceeding the criterion of $66\,\mu g\,m^{-3}$. This day belonged to the synoptic weather pattern known as "a cold front passage". The PM_{10} concentration consists of primary aerosol as well as secondary aerosol. To identify source–receptor relationship quantitatively, the back trajectories and contributed concentrations of PM_{10} are shown in Fig. 5a. The contributed PM concentration includes primary aerosol, sulfate, nitrate and ammonium. The open circles along the trajectory path indicate the directions and the locations of an air parcel at each hour. The stick on each of the circles shows the wind direction, and the small branches on the tail of a stick show its wind speed. The distance between two consecutive trajectory points is the distance wind traveled in 1 h. Shaded areas are the contributed concentrations of each grid in $1 \times 1\,km^2$ resolution.

At 3 a.m., wind was nearly calm and circulated around Taipei Basin. The PM_{10} concentration was over $150\,\mu g\,m^{-3}$ in stable weather conditions and nocturnal inversion. The major contributed concentrations of PM_{10} came from nearby sources in Taipei City within the region of $10 \times 10\,km^2$ centered on the receptor. They were mainly road dust and vehicle exhaust (CTCI, 1999). Highway 1, 20 km to the north, and one stationary source, Lin-Kou power plant, 25 km to the NWW from the receptor, were identified as major sources.

At 9 a.m., the air parcel entered Taipei Basin from the NW along a meandering trajectory to the receptor. The contributed concentrations along the trajectory in land were about $0.1–1\,\mu g\,m^{-3}\,km^{-2}$. Interestingly, the figure shows that sources in windward regions 7–11 h in advance of a receptor, where the wind speed was slow, had the highest contributed concentrations to the receptor. It shows a "teleconnection" between the source Highway 3, 20 km to the SWW, and the receptor. The contributed PM in this remote region was mainly nitrate aerosol converted from the emission of gaseous NO_x from the highway (Fig. 5b).

The back trajectories and contributed concentrations of CO are shown in Fig. 5c. In contrast to PM, the mechanisms involving the formation of CO only relate to the advection–diffusion mechanism. Unlike PM, there is no mechanism of transformation involved and no secondary CO exits. Hence, there is no "teleconnection" shown in the figure. The major contributed concentrations of CO came only from nearby sources in Taipei City within the region of $10 \times 10\,km^2$ centered at the receptor—mainly vehicle exhaust.

4.1.2. A non-episode day

Fig. 6 shows a contour of the contributed concentration for a non-episode day on 22 March 1998. On that day, PM_{10} daily average concentration was at a low value of $13\,\mu g\,m^{-3}$. This day belonged to the synoptic weather pattern known as "standard northeast monsoon", when the prevailing wind came from the NE throughout the day and wind speed was high. The major contributed concentrations of PM_{10} came from nearby sources in Taipei City within the region of $10 \times 10\,km^2$ with contributed concentrations of $0–0.3\,\mu g\,m^{-3}\,km^{-2}$ centered at the receptor—less than those on the episode day presented above.

4.2. Emission data and sounding data

There is always a request for a better data quality. Most frequently requested items include an emission inventory in time series and the availability of sounding data. Both of the data are relatively costly to procure. To evaluate their importance, the following tests are performed. First, we compare the calculated concentrations without using the DOWV in the emission inventory. The result is shown in Table 7, which shows that the model that took into consideration the DOWV of emissions improved the simulated results of the correlation coefficients. Second, we compare the calculated concentrations without using the sounding

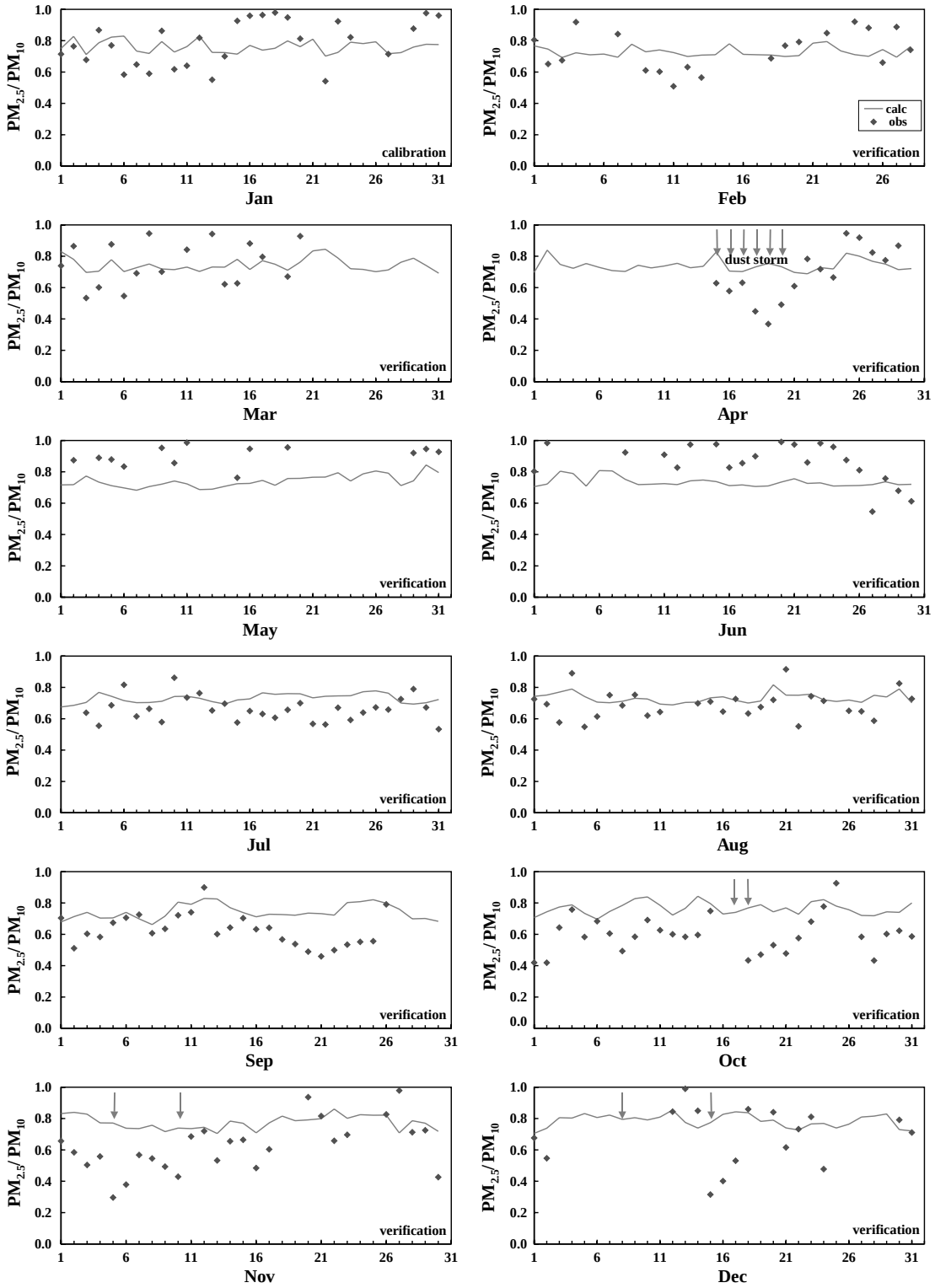

Fig. 4. The ratios of $PM_{2.5}$ to PM_{10} daily concentrations at Ku-Ting station, Taiwan, 1998. Arrows on the top of each graph represent Asia dust storm periods.

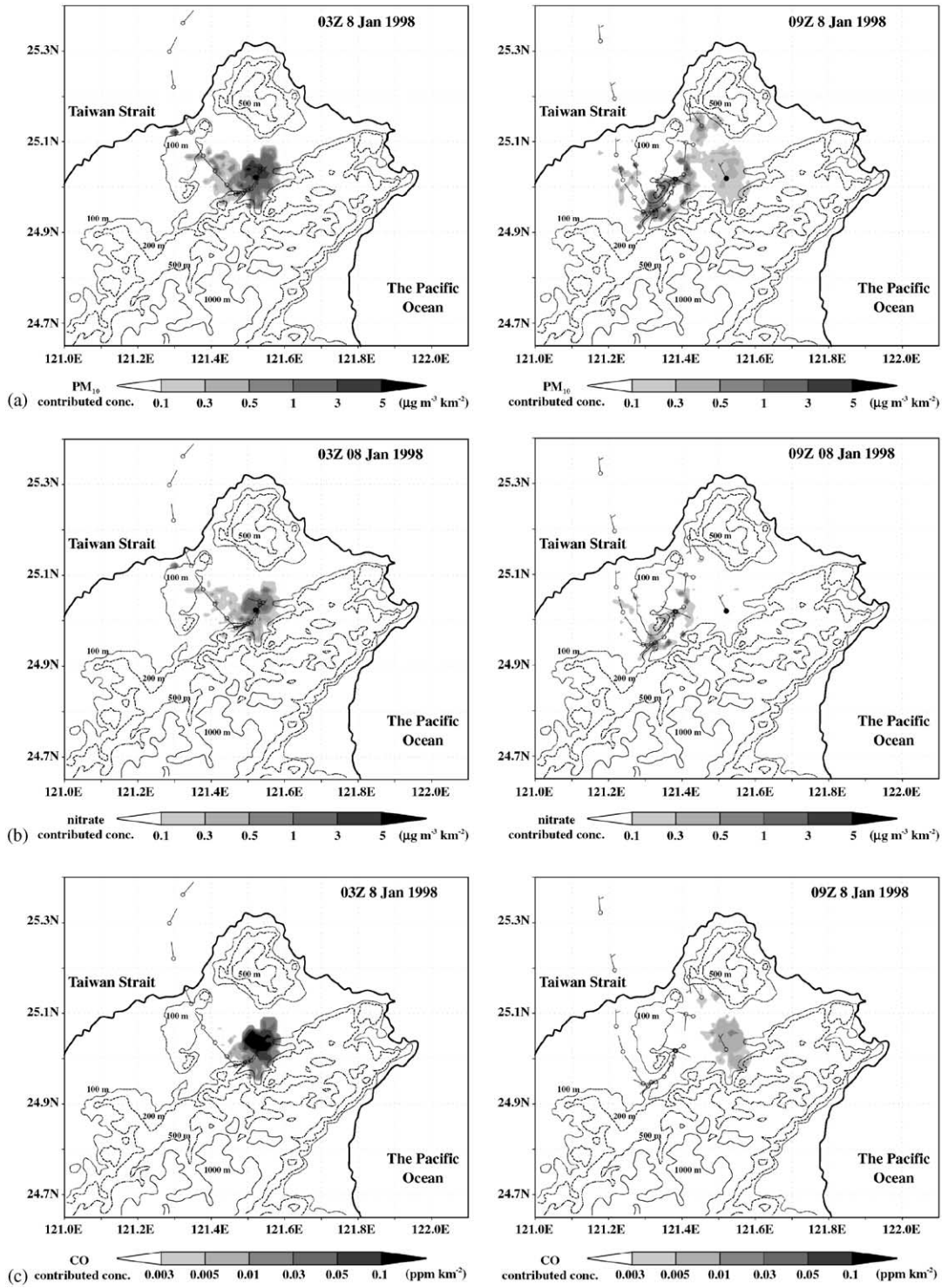

Fig. 5. Simulated (a) PM_{10}, (b) nitrate aerosol and (c) CO contributed concentrations on an episode day (8 January 1998). The receptor (solid circle) is Ku-Ting monitoring station. Contour lines represent the elevations.

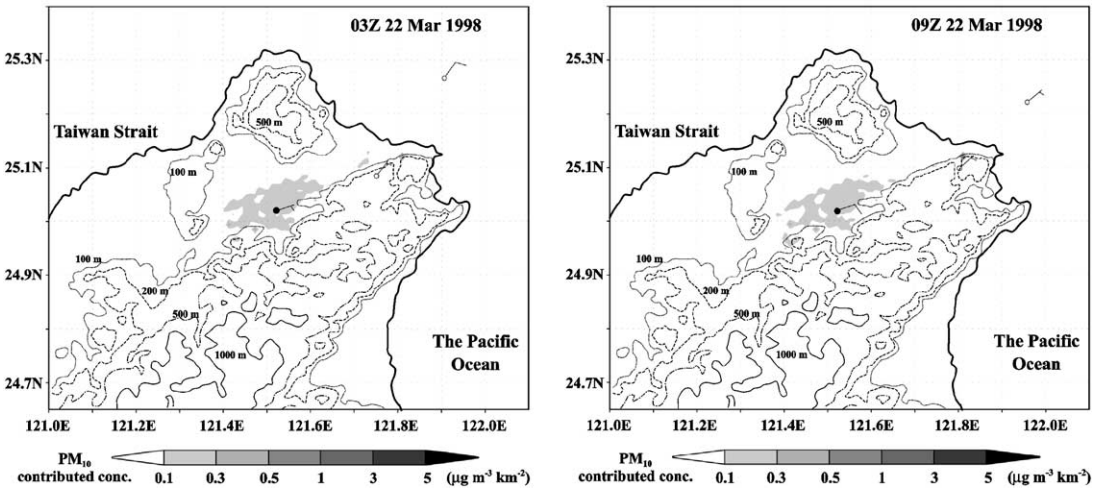

Fig. 6. Same as Fig. 5 except on a non-episode day (22 March 1998).

Table 7
Calculated results of three simulation conditions: base, no DOWV and no airsonde data[a]

Results	CO	NO_x	SO_2	$PM_{2.5}$	PM_{10}
Corr. coeff.					
Base	0.75	0.69	0.39	0.55	0.55
No DOWV	0.72	0.64	0.37	0.54	0.55
No airsonde data	0.74	0.68	0.33	0.53	0.56
EDR					
Base	87%	88%	85%	79%	83%
No DOWV	86%	87%	84%	77%	82%
No airsonde data	86%	87%	85%	81%	86%

[a] EDR: episode-distinguished ratio.

data for estimating the mixing height. If there is no airsonde data, the lapse rate above mixing height is fixed to be the wet adiabatic lapse. Table 7 also shows the results of the model using wet adiabatic lapse rate instead of observed airsonde data. The correlation coefficient between simulated SO_2 and observed data is worse. But, the results of PM_{10} are somewhat better than those results using airsonde data. Therefore, there is no significant improvement in using observed lapse rate than using wet lapse rate.

5. Conclusion

Although the current model is not as complete as some aerosol Eulerian models (Jacobson, 1997a, b; Lurmann et al., 1997; Nenes et al., 1999), the model is able to simulate the daily variation of PM concentration at a receptor. In addition, it is able to identify major sources of PM emission, SO_2 emission and NO_x emission contributing to the receptor with much smaller computational resources. The model takes cpu time of 263–367 s, varying with output options, for 30 days of simulation on a Pentium II 350 running Red Hat Linux 6.0. In contrast to UAM aero2 using ISORROPIA code for aerosol simulation, it takes 37,477 s of cpu time for 3 days of simulation over California's south coast air basin on an HP 9000/715 workstation running HP-UX 9.05 (Nenes et al., 1999). The notion of determining transfer coefficients by an air quality model is important for the design of a better abatement strategy. The idea of determining transfer coefficients has been used for receptor models to determine low-cost strategies for the reduction of PM concentrations at receptors (Cass and McRae, 1983; Tsuang and Chang, 1997). This model determines the transfer coefficients qualitatively and quantitatively in the angular resolution as well as in the radial resolution.

The model results contrasted with observations in an air quality station in Taipei City indicate that the

correlation coefficient for daily concentrations of CO, NO_x, SO_2, $PM_{2.5}$ and PM_{10} are 0.75, 0.69, 0.39, 0.55 and 0.55, respectively. Sensitivity analysis shows that the calculated concentrations are very sensitive to their dry deposition velocities. A more thorough study is suggested especially for that of $PM_{2.5}$. Note that the above correlation coefficients can be compared with statistical models. Tsuang (1993) derived a multiple-linear regression equation to correlate PM_{10} concentrations with meteorological factors with a correlation coefficient of 0.55 in Taipei. Ziomas et al. (1995) derived an equation to correlate daily maximum NO_2 concentration with meteorological factors and the previous day's maximum concentration with a correlation coefficient of 0.68–0.72 in Athens, Greece.

It is therefore believed that the use of the model together with other prognostic systems can be used for air quality prediction and may enable the responsible authorities to issue warnings and take restrictive measures in advance. The priority regions where these restrictive measures can be taken are shown clearly on plots of the contributed concentration maps such as Figs 5 and 6 simulated by the model. This model is available to the public on the Internet at "http::// air701.ev.nchu.edu.tw/ctx/" under the General Public License Agreements.

Acknowledgements

The author would like to acknowledge the support of this work by National Science Council, R.O.C., under contract NSC-88-2211-E005-018 and NSC-89-EPA-Z-005-004. Suggestions from Prof. Len-Fu W. Chang at Nat'l Taiwan Univ. are also appreciated.

References

Cass, G.R., McRae, G.J., 1983. Source–receptor reconciliation of routine air monitoring date for trace metals: an emission inventory assisted approach. Environmental Science and Technology 17 (3), 129–139.

Chang, S.C., Wu, C.F., 2001. The impact of dust storm on the air quality of Taiwan. Symposium on the Impact of Asia Dust Storm on the Air Quality of Taiwan and Prediction of these Events. Taipei, Taiwan, R.O.C., pp. 85–106.

Chang, W.-L., Cardelino, C., Chang, M.E., 1996. The use of survey data to investigate ozone sensitivity to point sources. Atmospheric Environment 30 (23), 4095–4099.

Chang, K.-H., Huang, H.-C., Chang, J.-S., 2000. Modeling approach for resolving the causes on high O_3 concentration in Central Taiwan. Abstracts of Seventh International Conference on Atmospheric Sciences and Applications to Air Quality, ASAAQ, 31 October–3 November 2000. Taipei, Taiwan, pp. 161.

Chate, D.M., Kamra, A.K., 1997. Collecting efficiencies of large water drops collecting aerosol particles of various densities. Atmospheric Environment 31 (11), 1631–1635.

Chen, T.J., Chen, H.J., 1987. Study on large-scale features of duststorm system. Meteorological Research 10 (1), 57–80.

Cheng, S., Lam, K.-C., 1998. An analysis of winds affecting air pollution concentrations in Hong Kong. Atmospheric Environment 32 (14/15), 2559–2567.

CTCI Corporation, 1999. Carrying capacity management plan for air pollutants and estimation of emission inventory over Taiwan. Environmental Protection Administration, R.O.C.

Draxler, R.R., 1987. Sensitivity of a trajectory model to the spatial and temporal resolution of the meteorological data during CAPTEX. Journal of Climate and Applied Meteorology 26, 1577–1588.

Environmental Protection Agency, United States (EPA/US), 1994. A revised user's guide to MESOPUFF II (V5.1). EPA-454/B-94-025. US Environmental Protection Agency. Research Triangle Park, NC.

Environmental Protection Agency, United States (EPA/US), 1995. User guide for the CALPUFF dispersion model. EPA-454/B-95-006. US Environmental Protection Agency. Research Triangle Park, NC.

Hertel, O., Christensen, J., Runge, E.H., Asman, W.A.H., Berkowicz, R., Hovmand, M.F., Hov, Ø., 1995. Development and testing of a new variable scale air pollution model-ACDEP. Atmospheric Environment 29, 1267–1290.

Holzworth, G.C., 1972. Mixing Heights, Wind Speeds and Potential for Urban Air Pollution Through Contiguous United States. AP-101, US EPA, Raleigh, NC.

Jacobson, M.Z., 1997a. Development and application of a new air pollution modeling system-II: aerosol module structure and design. Atmospheric Environment 31, 131–144.

Jacobson, M.Z., 1997b. Development and application of a new air pollution modeling system-part III: aerosol-phase simulations. Atmospheric Environment 31, 587–608.

Juozaitis, A., Tralcumas, S., Girgždienė, R., Girgždys, A., Šopauskienė, D., Ulevičius, V., 1996. Investigations of gas-to-particle conversion in the atmosphere. Atmospheric Research 41, 183–201.

Kahl, J.D., Samson, P.J., 1986. Uncertainly in trajectory calculations due to low resolution meteorological data. Journal of Climate and Applied Meteorology 25, 1816–1831.

Kessler, E., 1969. On the distribution and continuity of water substance in atmospheric circulation. Meteorological Monographs 32, 84.

Kuang, Y.-C., 2000. Secondary aerosol simulation over Taiwan. The Proceeding of 17th Air Pollution Control Technologies Conference, Yunlin, Taiwan, pp. 440–445.

Kuo, Yee-Ling, Wu, Yee-Lin, Chang, Len-Fu, W., 1996. The formation rate of secondary nitrate and sulfate in Southern Taiwan. The Proceeding of 13th Air Pollution Control Technologies Conference, Taipei, Taiwan, pp. 81–88.

Lurmann, F.W., Wexler, A.S., Pandis, S.N., Musarra, S., Kumar, N., Seinfeld, J.H., 1997. Modelling urban and regional aerosols-II. Application to California's south coast air basin. Atmospheric Environment 31, 2695–2715.

Ministry of the Interior, R.O.C. (MOI), 2001. http::// www.moi.gov.tw/.

Nenes, A., Pandis, S.N., Pilinis, C., 1999. Continued development and testing of a new thermodynamic aerosol module for urban and regional air quality models. Atmospheric Environment 33, 1553–1560.

Padro, J., Hartog, G.D., Neumann, H.H., 1991. An investigation of the ADOM dry deposition module using summertime O_3 measurements above a deciduous forest. Atmospheric Environment 25A, 1689–1704.

Rolph, G.D., Draxler, R.R., 1990. Sensitivity of three-dimensional trajectories to the spatial and temporal densities of the wind field. Journal of Applied Meteorology 29, 1043–1054.

Schwede, D.B., Paumier, J.O., 1997. Sensitivity of the industrial source complex model to input deposition parameters. Journal of Applied Meteorology 36, 1096–1106.

Scire, J.S., Robe, F.R., Fernau, M.E., Yamartino, R.J., 2000. A user's guide for the CALMET meteorological model (version 5). Earth Tech., Inc., Concord, MA.

Scott, B.C., 1982. Theoretical estimates of the scavenging coefficient for soluble aerosol particles as a function of precipitation type, rate and altitude. Atmospheric Environment 16, 1753–1762.

Seinfeld, J.H., Pandis, S.N., 1998. Atmospheric Chemistry and Physics from Air Pollution to Climate Change. Wiley, New York, 1057 pp.

Simmonds, I., Keay, K., 1997. Weekly cycles of meteorological variations in Melbourne and the role of pollution and anthropogenic heat release. Atmospheric Environment 31 (11), 1589–1603.

Slinn, S.A., Slinn, W.G.N., 1980. Predictions for particle deposition on natural waters. Atmospheric Environment 24, 1013–1016.

Stohl, A., 1998. Computation, accuracy and applications of trajectories—a review and bibliography. Atmospheric Environment 32, 947–966.

Tsai, Y.I., Cheng, M.T., 1999. Visibility and aerosol chemical compositions near the coastal area in Central Taiwan. The Science of the Total Environment 231, 37–51.

Tsuang, B.J., 1993. The correlation between Taipei metropolitan 8-AM PM10μ concentration and surface layer eddy diffusivity, wind speed, rain and mixing height. Journal of the Chinese Institute of Environmental Engineering 3, 95–102.

Tsuang, B.-J., Chang, L.-P., 1997. Ranking PM_{10} control strategies for Taichung city by nonlinear programming. Journal of the Chinese Institute of Environment Engineering 7 (2), 141–159.

Tsuang, B.-J., Chao, C.-P., 1999. Application of circuit model for Taipei City PM_{10} simulation. Atmospheric Environment 33, 1789–1801.

Tsuang, B.-J., Tu, C.-Y., 2001. Model structure and land parameter identification: an inverse problem approach. Journal of Geophysical Research, in revision.

Tsuang, B.-J., Huang, P.-L., Chen, C.-L., Lin, C.-S., Lin, H.-Q., Tsai, J.-L., 2000. Considering the channel effect of terrain in trajectory simulation. The Proceeding of 17th Air Pollution Control Technologies Conference. Yunlin, Taiwan, pp. 473–477.

Tsuang, B.-J., Chen, C.-L., Pan, R.-C, Liu, J.-H., 2002. Quantification the source/receptor relationship of primary pollutants and secondary aerosols from ground sources—Part I Theory. Atmospheric Environment 35, 411–419.

Tsuang, B.-J., Lin, C.-H., Chen, C.-L., Cheng, M.-T. Development of a Gaussian plume trajectory model incorporating the removal and the formation of secondary sulfate and nitrate. Environmental Science and Technology, submitted for publication.

Tu, C.-Y., 1999. Development of an integrated PBL and land model to simulate air temperature, Master's Thesis. Department of Environmental Engineering, Nat'l Chung-Hsing University, R.O.C.

Uijlenhoet, R., Stricker, J.N.M., 1999. A consistent rainfall parameterization based on the exponential raindrop size distribution. Journal of Hydrology 218, 101–127.

Wesely, M.L., 1989. Parameterizations of surface resistance to gaseous dry deposition in regional scale, numerical models. Atmospheric Environment 23, 1293–1304.

Wesely, M.L., Hicks, B.B., 2000. A review of the current status of knowledge on dry deposition. Atmospheric Environment 34, 2261–2282.

Yang, Y.-J., Wilkinson, J.G., Russell, A.G., 1997. Fast, direct sensitivity analysis of multidimensional photochemical models. Environmental Science and Technology 31, 2859–2868.

Ziomas, I.C., Melas, D., Zerefos, C.S., Bais, A., Paliatsos, A.G., 1995. Forecasting peak pollutant levels from meteorological variables. Atmospheric Environment 29 (24), 3703–3711.